Online tracking of the phase difference between neural drives to antagonist muscle pairs in essential tremor patients

N.B. When citing this work, cite the original published paper.

(article starts on next page)

Online Tracking of the Phase Difference Between Neural Drives to Antagonist Muscle Pairs in Essential Tremor Patients

Gonthicha Puttaraksa , Silvia Muceli , *Senior Member, IEEE,* Deren Y. Barsakcioglu, *Member, IEEE,* Ales Holobar , *Member, IEEE,* Alexander Kenneth Clarke , Steven K. Charles , José L. Pons , *Senior Member, IEEE,* and Dario Farina , *Fellow, IEEE*

Abstract—Transcutaneous electrical stimulation has been applied in tremor suppression applications. Out-of-phase stimulation strategies applied above or below motor threshold result in a significant attenuation of pathological tremor. For stimulation to be properly timed, the varying phase relationship between agonist-antagonist muscle activity during tremor needs to be accurately estimated in real-time. Here we propose an online tremor phase and frequency tracking technique for the customized control of electrical stimulation, based on a phase-locked loop (PLL) system applied to the estimated neural drive to muscles. Surface electromyography signals were recorded from the wrist extensor and flexor muscle groups of 13 essential tremor patients during postural tremor. The EMG signals were pre-processed and decomposed online and offline via the convolution kernel compensation algorithm to discriminate motor unit spike trains. The summation of motor unit spike trains detected for each muscle was bandpass filtered between 3 to 10 Hz to isolate the tremor related components of the neural drive to muscles. The estimated tremorogenic neural drive was used as input to a PLL that tracked the phase differences between the two muscle groups. The online estimated phase difference was compared with the phase calculated offline using a Hilbert Transform as a ground truth. The results showed a rate of agreement of 0.88 ± 0.22 between offline and online EMG decomposition. The PLL tracked the phase difference of tremor signals in real-time with an average correlation of 0.86 ± 0.16 with the ground truth (average error of $6.40° \pm 3.49°$). Finally, the online decomposition and phase estimation components were integrated with an electrical stimulator and applied in closed-loop on one patient, to representatively demonstrate the working principle of the full tremor suppression system. The results of this study support the feasibility of real-time estimation of the phase of tremorogenic neural drive to muscles, providing a methodology for future tremor-suppression neuroprostheses.

Index Terms—Tremor, essential tremor, phase-locked loop system, phase tracking.

Gonthicha Puttaraksa, Deren Y. Barsakcioglu, Alexander Kenneth Clarke, and Dario Farina are with the Bioengineering Department, Imperial College London, London W12 0BZ, U.K. (e-mail: g.puttaraksa17@ic.ac.uk; deren.barsakcioglu10@imperial.ac.uk; d.farina@ic.ac.uk).

Silvia Muceli is with the Department of Electrical Engineering, Chalmers University of Technology, 41296 Gothenburg, Sweden (e-mail: muceli@chalmers.se).

Ales Holobar is with the Faculty of Electrical Engineering and Computer Science, University of Maribor, 2000 Maribor, Slovenia.

Steven K. Charles is with the Department of Mechanical Engineering and Neuroscience Center, Brigham Young University, Provo, UT 84602 USA.

José L. Pons is with the Legs and Walking Ability Laboratory, Shirley Ryan AbilityLab, Chicago, IL 60611 USA.

Digital Object Identifier 10.1109/TNSRE.2022.3158606

I. INTRODUCTION

TREMOR is characterized by rhythmic oscillations of body parts around joints [1], [2]. It is a common phenomenon that is experienced by healthy individuals (physiological tremor) or by people with movement disorders, such as essential tremor (ET) and Parkinson's disease (pathological tremor). Physiological tremor is a low-amplitude and high-frequency oscillation ranging from 8 to 12 Hz [3], [4] and is inherently present in the activation of healthy muscles during voluntary contractions and in particular during fatigue. Unlike physiological tremor, pathological tremor has a broader frequency range (1 to 25 Hz) and higher oscillatory amplitude [5], [6]. This type of tremor is likely to be caused by abnormalities in either the central nervous system, peripheral nervous system, their pathways to muscles, or all of them together. The involvement of this assembled structure at different frequencies of tremor activities has been investigated using spectral coherence and phase analysis [7]–[13].

Among different types of pathological tremor, ET is the most common tremor disease, affecting 4% of people aged over 50 [14]. ET is characterized by postural tremor that occurs whilst maintaining a limb position against gravity [15] and kinetic tremor that occurs when a body part is moving [16], [17]. Although pharmacotherapy and deep brain stimulation surgery are the most common and effective treatments for pathological tremor, these approaches have several limitations and they are not always effective [18]. As an alternative, the tremor rhythm can be attenuated by apply-

ing mechanical perturbance [19], [20], transcranial magnetic stimulation [21]–[23], or electrical stimulation to peripheral nerves [24]–[27]. These techniques have been validated in subjects with physiological tremor, Parkinson's patients with postural tremor, and ET patients [19]–[21], [23]–[27]. Among these techniques, the use of electrical stimulation of peripheral nerves seems to be the most viable for a wide clinical/home use since it involves stimulation of distal parts of the body where it is less likely to cause discomfort or side effects.

Electrical stimulation is used to generate muscle activations by providing impulses that excite the nerves supplying muscles. Closed-loop electrical stimulation for tremor suppression has been implemented in association with various sensors, such as displacement sensors [28], inertial sensors [29], [30], and surface and intramuscular electromyography (EMG) [31]–[34]. In the literature several strategies have been proposed to achieve tremor control, such as simultaneous stimulation (to produce co-contraction of the antagonist muscles) [35] and out-of-phase stimulation [30], [31], [36] with currents either above or below the threshold for muscle activation [37].

Zhang *et al.* [32] demonstrated significant tremor suppression, using artificial EMG-regulated neuronal oscillators to control electrical stimulation, with stimulation parameters tuned by a proportional-integral-differential controller of motion signals. This technique achieved a 94% of tremor amplitude suppression but has not been practically validated in patients [32]. Maneski *et al.* [30] used an inertial sensor (gyroscope) to time the electrical stimulation in an out-of-phase manner and tested the system on healthy subjects, Parkinson's patients, and ET patients. Although a tremor suppression of 67% was observed, the phase tracking by motion sensors was associated with relatively large delays which would make practical adoption difficult.

Closed-loop systems for tremor suppression based on EMG have also been extensively investigated. Dideriksen *et al.* [31] and Dosen *et al.* [36] have shown that out-of-phase subthreshold stimulation (below the threshold of muscle activation) could reduce tremor, as measured by the oscillations of the affected joint (the wrist). Although the out-of-phase stimulation strategy produces significant levels of tremor attenuation, recent studies have demonstrated that the phase differences between a pair of antagonist muscle activities at the tremor frequency of 3 to 10 Hz varies greatly and rapidly over time [12], [38], meaning an accurate real-time estimation of muscle activity phase during tremor is needed for continuous control. For this reason, we propose a system for real-time estimation of the phase difference in the neural drive to agonist and antagonist muscles during tremor. The neural drives are estimated by online decomposition of high-density EMG signals into individual motor units (MUs) because they are the best representatives of the neural command from the central nervous system through their pathways to muscles [9], [38], [39]. The phase of the neural drives is tracked by a phase-locked loop (PLL) system and used to control the stimulation timing. We provide extensive results on validation of all parts of the system, both offline and online on patients' data. Following this validation, we show the working principle of the full system in closed-loop in one ET patient, as a proof-of-concept demonstration.
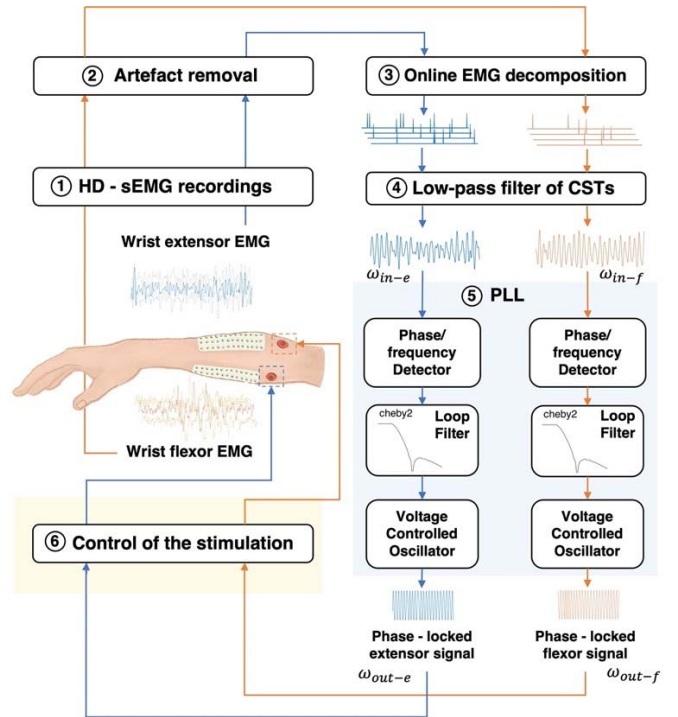

Fig. 1. Closed-loop tremor suppression system flow chart.

II. MATERIAL AND METHODS

A. Patients

Data for the validation of the system components were recorded from 13 ET patients (5 women; age 68.9 ± 0.8 yrs) with a diagnosis of ET according to the Movement Disorder Society consensus criteria [2]. All patients had a prominent postural forearm tremor, at grade 2 - 4 on the Fahn - Tolosa - Marin tremor rating scale. Tremor severity in the most affected limb was 28.9 ± 10.3 (ranging from 10 to 51). Average disease duration was 17.3 ± 9.5 yrs, ranging from 2 to 43 yrs. Seven patients had left tremor predominance, five patients had right tremor predominance and one patient had bilateral tremor. Three of the patients were not on medical treatment while the rest of the patients used medications to treat tremor. All the patients were asked to discontinue their treatment prior to the experiment and none of them had been treated with deep brain stimulation. Following the validation of all system components on the 13 patients, an additional ET patient (male, 79 yrs) with prominent postural forearm tremor on the right side was recruited for the proof-of-concept real-time demonstration of the full closed-loop tremor suppression system. All procedures were approved by the Ethical Committee at the University Hospital "12 de Octubre" (Madrid) (for the tests on the 13 patients) and by the Imperial College Ethical Committee (for the proof-of-concept demonstration), in compliance with the Declaration of Helsinki. Written and signed informed consent was obtained from all study participants.

B. Closed - Loop Tremor Suppression System

Fig. 1 illustrates the process of estimating the phase difference of an antagonist pair of muscle activity to control the timing of electrical stimulation using cumulative spike train.

The process includes high-density surface EMG recordings from the extensor and flexor muscle groups (1), blanking of the stimulation artefact (2), online EMG decomposition using the convolution kernel compensation algorithm (3), low-pass filter of the cumulative spike trains (4), phase estimation using a phase-locked loop (PLL) system (5), and stimulation controller (6). The EMG signals from the two muscle groups were separately decomposed into MU spike trains before summation to create the cumulative spike trains and low-pass filtered at the tremor frequency (3 to 10 Hz). The phases of these filtered signals were then estimated using a PLL system which generated phase-locked signals of both muscles. Finally, the phases of the signals were used to control the stimulator in an out-of-phase manner. Specifically, the stimulation for the extensor muscle group was timed based on the phase of the flexor muscle activity and vice versa.

C. EMG Recording and Decomposition

For offline validation of the system, recorded tremor data were used to assess the accuracy of the proposed online decomposition and the phase-locked loop system. During the recording, the patients were seated on a comfortable armchair with their forearms fully supported. Postural tremor was provoked by asking the patients to stretch their dominant hand against gravity. Two 30-s recordings of 64 channels of the EMG data (grids of 13 x 5 electrodes -1 missing at the corner, inter-electrode distance 8 mm, single differential configuration) were acquired (EMG-USB2; OT-Bioelettronica, Italy, 2048-Hz sampling frequency and 12-bit analog-to-digital conversion) from the extensor and flexor muscle groups, providing 26 data sets from 13 patients.

The multi-channel EMG signal (X_i) can be mathematically described as a convolutive mixture of the impulse responses of filters representing motor unit action potential (MUAP) shapes, h_{ij} with a series of MU discharge timing (MU spike trains, S_j) as described in (1) [40].

$$X_i(n) = \sum_{j=1}^{N} \sum_{l=0}^{L-1} h_{ij}(l) S_j(n-l), \quad i = 1, \ldots, M \quad (1)$$

where N and M are the number of MUs (sources) and EMG channels, respectively. From this model, the MU spike trains (S_j) were discriminated from the EMG signals using the convolution kernel compensation decomposition algorithm [41]–[43].

S_j was calculated using the correlation matrix of the extended (delayed repetitions) observations (EMG signals) [42], and the cross-correlation vector between the EMG signals and the estimated MU spike trains. The product of the cross-correlation vectors and the correlation matrix were multiplied by the extended EMGs yielding MU spike trains [42, eq(17)]. In the offline decomposition, cross-correlation vectors were calculated from the whole recording period whereas for the online decomposition they were initialized from the first 10 s of the 30 s-long EMG recordings and applied to the remaining 20 s for online validation [40].

We have assessed that 10 s is a sufficient period for estimating the MUAP shapes of individual MUs of tremor EMGs as the spike triggered averaging [44] of the first 10 s or the whole
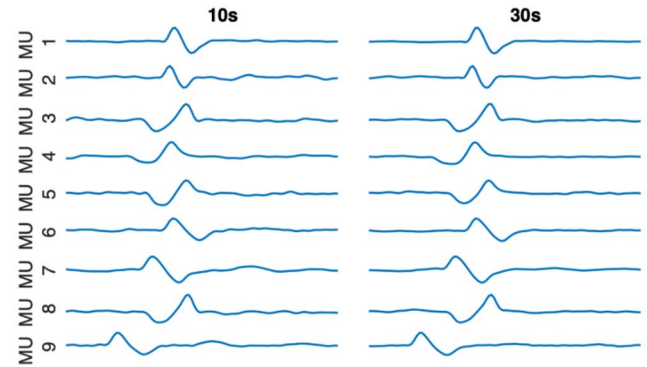

Fig. 2. Representative example of a comparison of the MUAP shapes of extensor muscles detected using the first 10 s-long EMG signals and the whole length of the signals (30 s). The MUAP shapes detected using 10 s were similar to those detected from the 30 s – long signals.

30 s of data yielded similar multi-channel MUAP templates (Fig. 2). The likelihood of estimated MU spike trains to be genuine were estimated using a validated metric, the pulse-to-noise ratio (PNR) [45]. Although PNR value of 30 dB is recommended for identification of individual MU spike trains [40], we accepted the spike trains with PNR $\geq$ 26 dB. Namely, we were not using individual spike trains in this study. Instead, all of the retained MU spike trains of each muscle were summed to create cumulative spike trains. Note that the quality of cumulative spike trains increases with the number of included MUs [46], whereas slightly increased rate of errors in estimation of individual MU discharges was not detrimental for the performance of our phase-locked loop system. The cumulative spike trains were then bandpass filtered (third-order Butterworth) at 3 to 10 Hz to isolate the tremor-related components of the neural drive [12].

D. Phase-Locked Loop (PLL) System

PLL is a feedback system capable of synchronizing phase and frequency of two waveforms. It consists of three components: a phase/frequency detector, a low-pass filter, and a voltage control oscillator (VCO). The PLL tracks phase and frequency shift of an input signal by proportionally varying the frequency of the VCO to match the input frequency which, thereby, induces phase locking between them.

There are several models of the PLL such as the linearized PLL which is the simplest model (used for example in [47]) and the digital charge pump PLL which is modified by replacing one or more components with digital circuitries. In this study, we used a digital charge pump PLL due to its large capture phase range (up to 4π) and the use of edge-triggered flipflop which produces no phase offset and makes the system insensitive to duty cycle of input signals [48].

Specifically, the phase and frequency of the filtered cumulative spike trains were identified by a tri-stage detector which differentiates the zero-crossing state of the input (cumulative spike trains) signal and the signal estimated from the VCO which initially generates synthesized signal at the quiescent frequency (Q_s). The state difference was then multiplied with the pump current gain (I_P) to produce a sequence of control voltage that adjusts the Q_s and minimizes the phase error
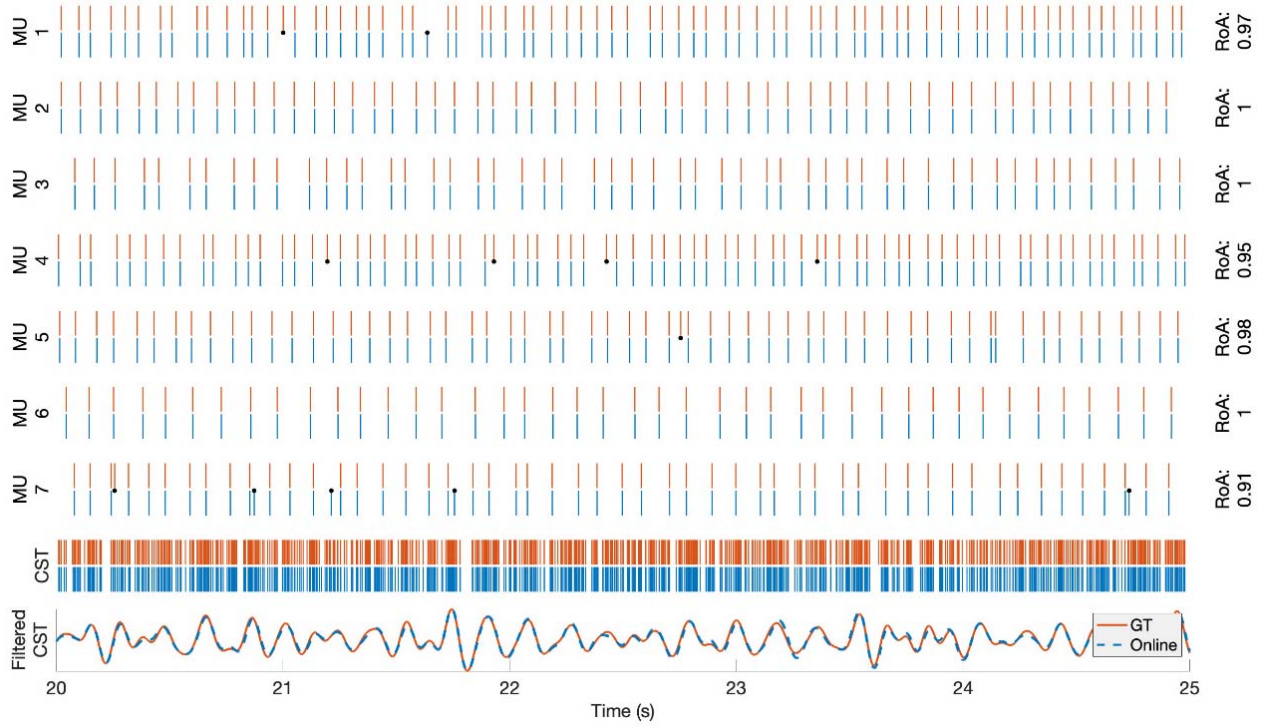
Fig. 3. The first seven panels depict representative examples of 7 individual MU spike trains identified by the offline decomposition (red line) and online decomposition (blue dashed line) from extensor muscles. The following panels are their cumulative spike trains and the filtered cumulative spike trains at 3 to 10 Hz, respectively. Each vertical line represents an MU discharge and disagreements between the online and offline decomposition are denoted by small black dots. The RoAs indicate the similarity of the discharge of each MU between offline and online decomposition.

between the cumulative spike train signal and the estimated signals until their phases are locked. In order to reduce the ripple of the logical control voltage signal (V_{cont}) and discard its harmonics, the V_{cont} was low-pass filtered using a Chebyshev filter (type II, third order). The linear function which relates the VCO output frequency to V_{cont} is

$$\omega_{out}(t) = Q_s + K_{vco}V_{cont}(t), \qquad (2)$$

where K_{vco} is the VCO sensitivity in radian/second/volt.

The charge-pump PLL was simulated in MATLAB Simulink (2020b). The Q_s and the K_{vco} of the PLL were simulated using Mixed-Signal Blockset. These parameters were determined to allow the VCO to vary its frequency around the tremor frequency range of 3 to 10 Hz. The following specific values were selected: low-pass cut-off frequency = 18 Hz, VCO gain = 0.4, $I_p = 1$, $K_{vco} = 3.5$ radian/second/volt and $Q_s = 6.5$ radian/second. The same parameters were used for all the data sets.

E. Proof-of-Concept Demonstration of the Online Tremor Suppression System

Following the extensive offline and online validation, the proposed system was further tested on one ET patient in closed loop. EMG high-density electrode type and position follow the description in Section II-C. A portable multichannel amplifier (Quattrocento, OT Bioelettronica, Italy) was used to acquire the EMG signals, which were amplified with gain of 150, sampled at 2048 Hz, and AD converted on 16 bits. The stimulation was delivered online with the stimulation timing corresponding to the phase of the neural drive to its antagonist

muscle to counteract tremor. The stimulation artefacts that contaminated the EMGs were blanked before the decomposition and phase estimation processes. The threshold for the artefact removal was set at 95% of the average artefact peaks in the first 2 s of the recordings obtained during stimulation. Twenty-five samples of EMG (5 before and 20 after the artefact peaks) were blanked. Blanked EMG recordings were then decomposed online to extract MU spike trains.

During the real-time proof-of-concept demonstration, a dual-phase approach to online decomposition was used [49]. During the training phase, the subject was provided with visual feedback using the average of the root mean square amplitude of all the EMG channels (128 channels). The subject was seated in a comfortable position (with elbow supported) and the forearm in postural position. The training phase started with estimation of the maximum voluntary contraction during a palmar grasp. The subject was then presented and asked to follow (by performing a palmar grasp) a 4-s ramp trajectory (3.75% MVC/s) followed by a 45 s constant trajectory at 15% of the MVC. The data acquired during the training phase was then used to compute the real-time decomposition parameters. The rationale for choosing the palmar grasp during training was to co-activate both extensor and flexor muscle groups allowing the simultaneous training of the agonist and antagonist muscles. During the online decomposition phase, the subject was provided with the real-time raster plots of the MU spiking.

EAST, a portable multichannel stimulator (OT Bioelettronica, Italy) was used to deliver positive electrical pulses with 300 μs pulse width and 100 Hz frequency [36]. Two circular

ValuTrode cloth neurostimulation electrodes (3.2cm Ø) were attached close to the later epicondyle of the elbow and proximal to the elbow crease to stimulate the extensor muscle and flexor muscle groups, respectively [36]. A rectangular cloth neurostimulation electrodes (5cm x 9cm) was positioned over the olecranon to act as common anode. To determine electrode positions prior to the start of the experiment, a sponge-attached stimulation electrode was slightly moved around the areas to determine where the motor response, slight flexion and extension of the wrist, could be activated. The stimulation frequency was set to 100 Hz and the pulse width to 300 μs as during the probing phase. As afferent stimulation (below the motor threshold) is as effective as motor stimulation (above the motor threshold) in suppressing tremor [36], we opted for afferent stimulation that prevents muscle fatigue and discomfort for the patients. The intensity of the stimulation was gradually increased from 1 mA in 1 mA step to determine the motor threshold. The intensity 1mA below this motor threshold was selected for the afferent stimulation. In this study, the intensity used for the extensor and flexor muscle stimulation was 14 mA and 8 mA, respectively.

The signal outputs (estimated phase of the filtered cumulative spike train during tremor) from the PLL were used to control the stimulation in an out-of-phase manner. Specifically, the estimated phase of the flexor muscle activity was used to time the stimulation of the extensor muscle group and vice versa. Each stimulation was activated when the instantaneous phase of the signal output was larger than 63° (70% of the PLL output amplitude). The activation of the stimulation, therefore, was adjusted according to the phase of the muscle activity. If the phases of the muscle activity from the extensor and flexor muscles was fully overlapped, the stimulation was not activated.

F. Data Analysis

Decomposition accuracy was validated on the pre-recorded data of the 13 patients. We assessed the accuracy of the online EMG decomposition on the tremor recordings by comparing their extracted MU spike trains with those decomposed from the offline decomposition using the Rate of Agreement (RoA) metric [40]

$$RoA_j = \frac{C_i}{C_j + A_j + B_j} \qquad (3)$$

where C_j is the number of discharges of the j MU spike train that was identified by both decompositions (tolerance set to 0.5 ms), A_j is the number of unmatched discharges of the j MU spike train identified from the offline decomposition and B_j is the number of unmatched discharges identified by the online decomposition.

The performance of the PLL was validated using the cumulative spike trains decomposed from the online and offline techniques. The groups of MU spike trains extracted from both techniques were used as inputs of the PLL system to assess their phases. The PLL separately estimates the phase of antagonist pair of muscles (extensors and flexors) before their phases were subtracted to obtain the *estimated phase difference* (PD_{EST}).
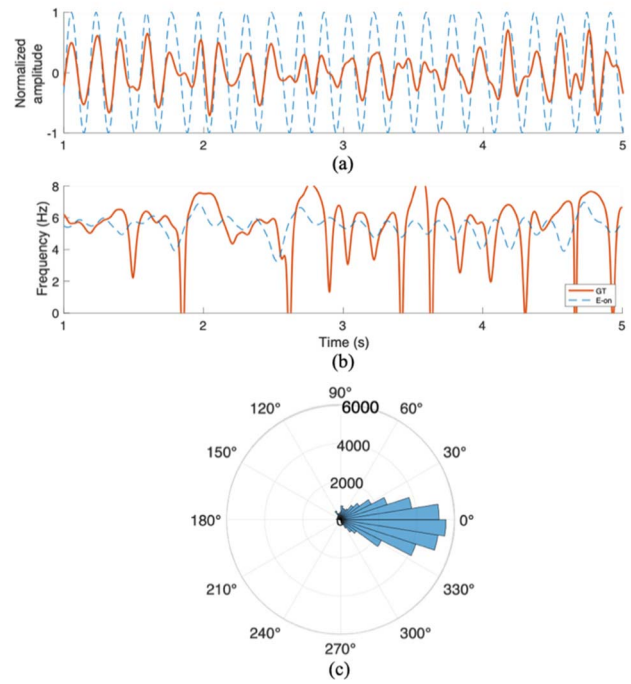

Fig. 4. Comparison of the estimated signal with the reference extensor signal of MU spike train decomposed online of a representative patient (a). The instantaneous frequency of the estimated signal and the reference is shown in b. The circular histogram shows the error between the $\varphi_{E\text{-}on}$ and the φ_{GT} of the extensor signals (c). The estimated signal shows high instantaneous frequency correlation value of 0.89 and difference in phase compared to the φ_{GT} concentrated at - 0.99° showing the ability of the PLL in tracking the frequency and the main phase of individual muscle activations.

To evaluate the system performance in tracking the agonist-antagonist phase difference, a *ground truth phase difference* (PD_{GT}) is required for the comparison. The PD_{GT} was calculated offline from the Hilbert Transform, a commonly used technique to calculate phase [29], [50], from 30 s-long cumulative spike trains of antagonist muscle pairs decomposed offline and filtered at the tremor frequency. We used the MU spike trains decomposed using the offline convolution kernel compensation method as the ground truth to calculate the PD_{GT} because this technique has been validated with simulated tremor signals with added voluntary movement and experimental data from Parkinson's patients and ET patients performing isometric contractions [51]. This technique has high accuracy in decomposing simulation signals compared with their reference and is able to identify the main characteristics of tremor-related MU activity similar to the observation via intramuscular EMG recordings [52], [53].

The correlation between the PD_{EST} (using offline or online decompositions) and the PD_{GT} was then calculated using cross-correlation analysis. Circular histograms with 40-bin were used to plot the PD_{EST} and PD_{GT} and the error between them. The mean phase difference and their standard variation were compared.

For the proof-of-concept demonstration, the experiment started with 30s of baseline (stimulation off) followed by 30 s of stimulation on and repeated for 5 trials for each condition.
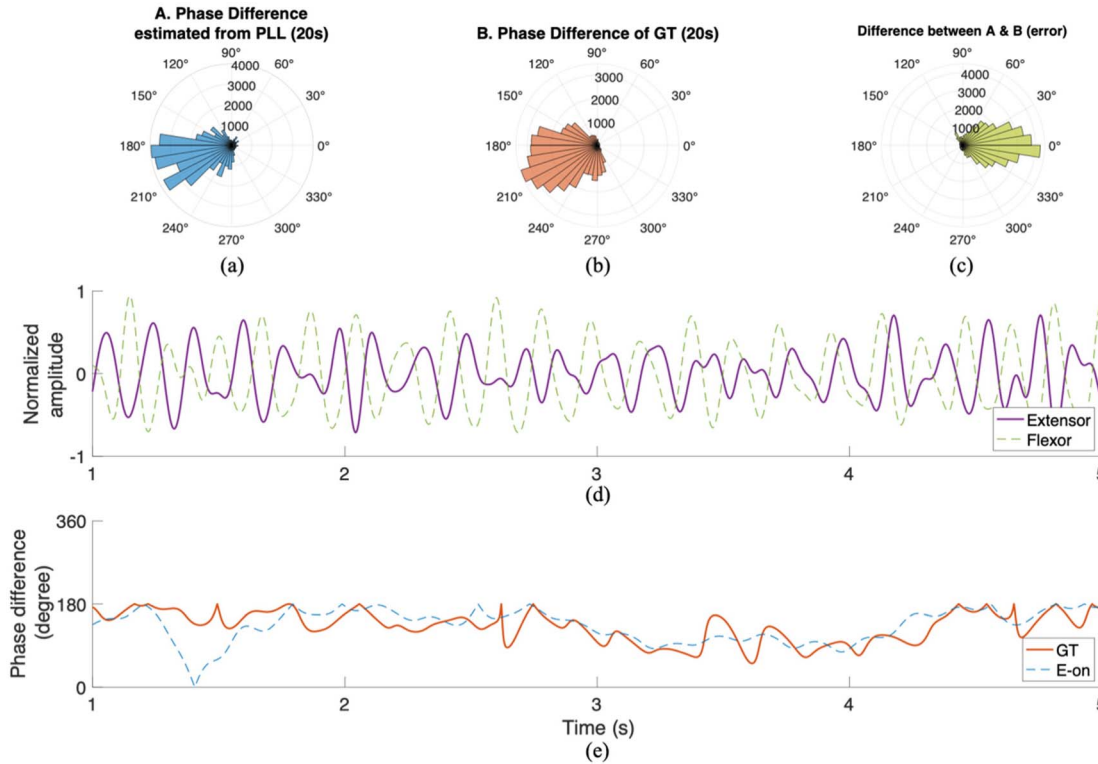
Fig. 5. The circular histogram shows the antagonist phase difference of the ground truth (PD_{GT}; a) and the estimated phase difference from the PLL ($PD_{E\text{-}on}$; b). The error between the PD_{GT} and $PD_{E\text{-}on}$ was shown in (c). The small difference between the PD_{GT} and the $PD_{E\text{-}on}$ indicates that the phase of the PLL estimated signal is similar to the GT. Panel d depicts the tremor signals of extensor (purple line) and flexor (green dashed line) muscle groups. Panel e shows the comparison of PD_{GT} (red line) and $PD_{E\text{-}on}$ (blue dashed line).

To assess the tremor during the stimulation as well as no-stimulation phases, a camera system was used. Three green markers (1.2cm × 1.2cm) were attached to the ulnar head of the fifth metacarpal bone (M1), the ulnar styloid process (M2), and in correspondence of the ulnar bone, 1/3 of the forearm distally (M3). A custom script written in Python 3.8 was used to manage video capture (30 frames per second) and marker position recognition for later post-processing to compute the wrist joint angle. The wrist flexion/extension angle was estimated as the acute angle between the directions identified by (M1, M2) and (M2, M3).

G. Statistical Analysis

The normality of variables including the average phase difference and the correlation values were visually observed using histogram plot and assessed using the Shapiro–Wilk test. To compare the estimated variables with their ground truths, pairs of normally distributed variables were compared using paired t-tests, whereas the Mann–Whitney–Wilcoxon test was used to compare non-normal data. The correlations between two variables were measured using the Pearson's correlation test for normally distributed data and the Spearman's correlation test for non-normal data. In all cases, the null hypothesis was rejected for P-values < 0.05. The results are represented as means $\pm$ SD and median (IQR).

III. RESULTS

A. Validation of the Online Decomposition

Decomposition accuracy was validated on the pre-recorded data of the 13 patients, which were processed simulating an online decomposition. The total number of identified MUs for offline and online identification (MU tracking with PNR > 26 dB) were 11.6 ± 5.2 and 10.8 ± 5.5 for extensor muscles, and 4.9 ± 2.6 and 4.7 ± 2.4 for flexor muscles, respectively.

Fig. 2 shows the MUAP shapes of the MUs decomposed in the first 10 s of a representative subject and the MUAP shapes of the MUs decomposed from the whole duration of the signals. The mean discharge rates were 11.4 ± 2.3 Hz and 11.5 ± 2.8 Hz for the MUs decomposed offline and online, respectively. The averaged RoA was 0.88 ± 0.22 across all the MUs detected from both algorithms. Across patients, the mean tremor frequency as estimated by the power peak frequency of power spectrum density within the tremor frequency range (3 to 10 Hz, Welch's method) was 6.8 ± 0.9 Hz, ranging from 5.5 to 8.8 Hz.

Fig. 3 illustrates a subset of the identified MU spike trains using online and offline decompositions and their cumulative spike train of extensor muscles of a representative subject. The vertical lines indicate the discharges of each MU and the dots denote disagreement of the discharges.

B. Validation of the PLL System

Hereafter, the ground truth variables will be indicated with the subscript 'GT' and the estimated variables with the subscript 'E'. We will add 'off' and 'on' for the variables estimated from the MU spike train decomposed offline and online, respectively. Note that the figures show the comparison of analysis obtained from the cumulative spike train decomposed online and the GT. The comparison of the analysis obtained
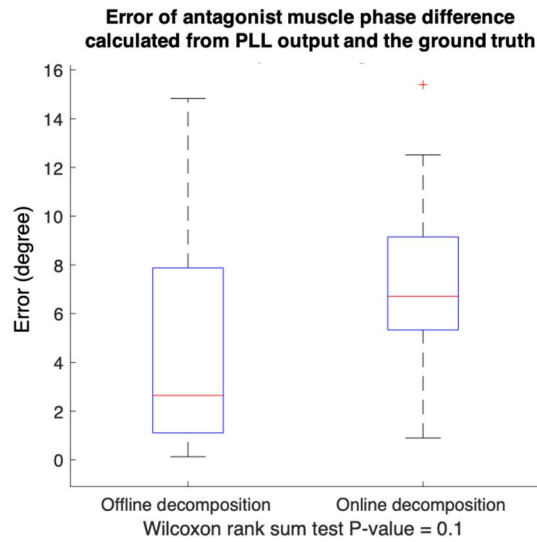
Fig. 6. The error between the estimated phase difference from the PLL using MU spike trains decomposed from the offline and online techniques, and the phase difference of the ground truth signals calculated using the Hilbert transform. The P-value of 0.1 (Wilcoxon rank sum test) shows no significant difference in the use of offline or online decomposed MU spike trains in estimating the antagonist muscles phase difference via PLL.

from cumulative spike train decomposed offline with the GT can be found in the text.

1) Performance of PLL in Detecting the Phase of Neural Drive in Individual Muscles: Phase estimates for individual muscles were assessed to ensure that the PLL could follow the frequency and phase of the reference signals. Fig. 4a illustrates the reference signal (red line) and the estimated signal from the PLL (blue dashed line) of the extensor muscle group of a representative patient. In theory, the phase of two signals will be locked when the frequencies of the two are equal. We have assessed the instantaneous frequency of the estimated signal to investigate if the PLL could follow the changes of the reference instantanous frequency (ω_{GT}) within the tremor range. The median of the correlation with the ω_{GT} of both muscles was 0.86 (0.17) and 0.86 (0.11) for ω_{E-off} and ω_{E-on}, respectively. This shows high similarity of the estimated instantaneous frequency and the ground truth. Fig. 4b shows the comparison of the ω_{E-on} (blue dashed line) with their ω_{GT} (red line) of the same muscle. Similarly, the correlation of instantaneous phase of all patients compared with the GT were 0.88 (0.09) and 0.88 (0.08) for φ_{E-off} and φ_{E-on}, respectively. The circular histogram shown in Fig. 4c, illustrates high similarity between φ_{GT} and φ_{E-on}.

2) Performance of PLL in Tracking the Phase Difference Between Neural Drives to Antagonist Muscle Pairs: The phase difference (PD) between the activations of antagonist muscle pairs was calculated by subtracting the instantaneous phase of extensor with those of flexor muscles. We assessed the performance of the PLL in estimating the phase difference by calculating the correlation between the PD_E and the PD_{GT}. Fig. 5 illustrates the circular histograms of the antagonist PD_{E-on} (a) and PD_{GT} (b), respectively, whereas the differences between them is shown in Fig. 5c. Fig. 5d shows the ground truth extensor and flexor muscle activities reflecting the
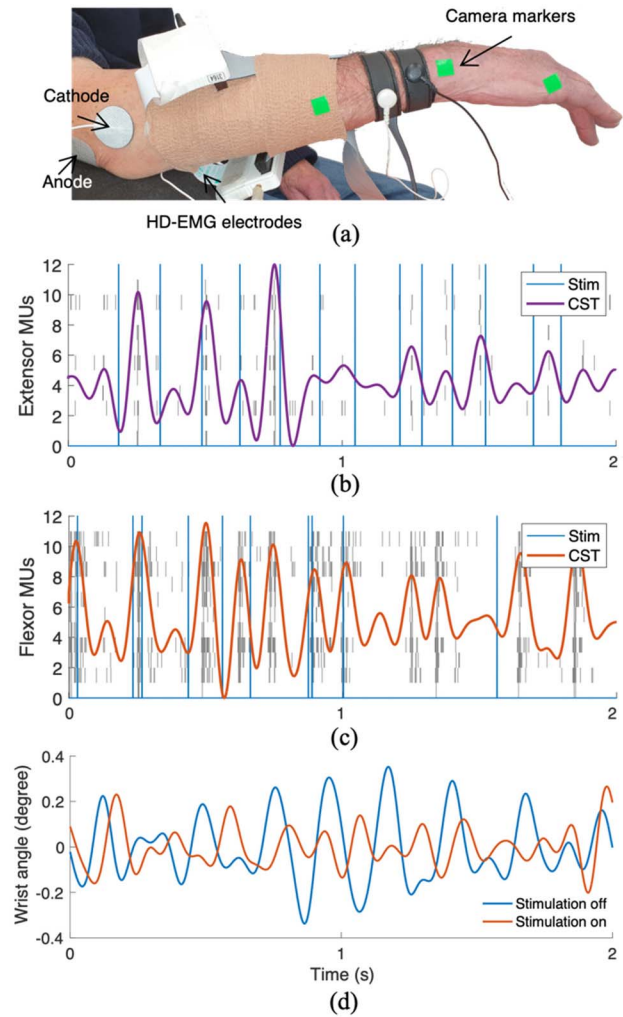
Fig. 7. Example of discharge timings of 12 and 11 identified MUs (gray lines) with corresponding cumulative spike trains from extensor (b) and flexor (c) muscles. The stimulation timings are indicated by the vertical lines. The wrist angles in two representative intervals of stimulation off (blue line) and on (red line) are compared in (d) and the positions of the electrodes and markers are shown in (a). Note that the plots of discharge times are not aligned to those of wrist angle (all of them are representative plots extracted from different intervals during the proof-of-concept experiment).

alternate bursts of tremor-related activations of the antagonist pair of muscles. A relatively low difference (error) between the PD_E and the PD_{GT} of 6.10° and a correlation of 0.95 indicated a high similarity between them.

The time-varying PD_{GT} (red line) and PD_{E-on} (blue dashed line) were compared in Fig. 5e. The median of the absolute error and the correlation values across all subjects were 2.32° (6.77°) and 0.90 (0.12), respectively, for the estimation using MU spike trains decomposed offline and 6.40° (3.49°) and 0.86 (0.16) for the estimation using MUs from online decomposition technique. Statistical analysis showed that the estimates of phase difference using either online or offline techniques were not significantly different (P-value = 0.1, Wilcoxon rank sum test, Fig. 6). However, the phase difference showed no significant correlation between offline and

online decomposition (R = 0.52, P-value = 0.07, Spearman's correlation test).

3) Proof-of-Concept Demonstration of the Online Tremor Suppression System: The system was preliminarily tested online on an ET patient. Fig. 7a illustrates the patient's forearm with HD-EMG matrix, stimulation electrodes and three markers on. The tremor frequency was 5.5 ± 1.4 Hz (average of the frequency corresponding to the peak of the power spectral density of the cumulative spike train filtered in the bandwidth 3 to 10 Hz across the 5 "stimulation off" trials). 21 and 11 MUs were decomposed from extensor and flexor muscles with firing rates of 11.7 ± 2.9 and 11.8 ± 2.5 pulse per second, respectively. Fig. 7 shows the cumulative spike trains decomposed online and the stimulation timings to extensor (b) and flexor (c) muscles during the "stimulation on" condition. The wrist angle is qualitatively compared for the case of stimulation and absence of stimulation in Fig. 7d. Overall, the closed-loop online test preliminarily demonstrated the potential and feasibility of the full recording system. While it is not possible from these representative results to draw conclusions on the level of tremor suppression, the provided demonstration shows that all system parts correctly work when applied in conditions similar to the target clinical application.

IV. DISCUSSION AND CONCLUSION

We have presented a real-time system (EMG decomposition followed by PLL on cumulative spike trains) that estimates the phase difference over time between tremorogenic neural drives to agonist-antagonist muscle pairs. This system can be used to drive electrical stimulation in closed loop to suppress tremor.

Various tremor suppression systems have exploited mechanical and inertial systems [29], [30], as well as EMG recordings [31]–[34], in order to tune the stimulation parameters (e.g. timing and frequency). Although the surface EMG enhances the accuracy of stimulation timing, estimating the phase of the signal from the surface EMG might not be reliable since it is not a perfect representative of the neural activation to the muscles [39], [54]–[56]. A better control of the stimulation parameters can be obtained by accurately identifying the discharge timings of MUs found by applying blind source separation algorithms to high-density surface EMG [42], [43], [57]–[61]. In this study, the validated offline [42], [61], [62] and online convolution kernel compensation decomposition [40] were used to discriminate the spike trains of each MU from the EMG of ET patients. The results show that the online decomposition has equivalent performance to the offline decomposition as calculated by the popular convolution kernel compensation source-separation algorithm. It is worth noting that the online decomposition was previously validated with data recorded from healthy subject [40] and the MU activities during tremor are highly correlated due to enhanced short-term synchronization [51]. Therefore, a further validation of online decomposition in data collected from this patient population was missing and it was carried out in this study.

In order to track the phase of muscle activity during tremor, a PLL (which is generally used to synchronize phase and frequency of two waveforms) was implemented and tuned by the discharge timing of the decomposed MU spike trains. Compared with the phase calculated offline using the Hilbert transform, the PLL provided highly accurate tracking of the phase difference. The PLL was also able to provide comparable estimation using either MU spike train decomposed offline or online to estimate the phases (no significant difference in the average phase difference of the estimated and the ground truth).

The advantage of implementing the PLL in the tremor suppression system is its ability to continuously produce a voltage oscillation closely following the phase of the reference tremor signals in real-time, as well as strictly following the frequency of the reference signals in a predefined frequency band (in this case, the tremor frequency between 3 and 10 Hz).

This ensures that only the tremor-related components of the reference signal are tracked and used to activate an electrical stimulator. This voltage oscillation signal could be used in real-time to modify the stimulator activation timing. A challenging limitation of PLL in tracking the phase is that the control signal produced by the PLL starts its phase at a pre-defined angle and needs a few milliseconds to adjust its initial phase to match the reference signal. Specifically, if the tremor oscillates at around 6 Hz, which is equivalent to 0.16 s per cycle, the PLL will need at least this time to change its frequency in order to follow the phase of the reference signal in a following waveform. This may have an effect when designing the stimulation of the tremor suppression system, as operation needs to be divided into stimulation periods and recording periods due to unavoidable stimulation artefacts in the EMG signal [31], [36]. To overcome this limitation, we have integrated the blanking algorithm to the EMG before the decomposition. For every stimulation pulse, 25 samples of the EMG were blanked. As the decomposition template was created during the training phase when the stimulation is not activated, the blanking did not significantly affect the performance of the decomposition. This allowed the same number of MUs to be identified between the training, "stimulation off" and "stimulation on" and the burst of the tremor to be distinguished. The full closed-loop system was tested on only one ET patient. For this patient, the proposed system worked correctly in all parts. However, the reduction of tremor varied among trials as the patient had very mild wrist tremor with intermittent tremor absence during the recordings. Therefore, it is not possible to draw general conclusions from this result. Nonetheless, the proof-of-concept demonstration showed the proper functioning of the system in a relevant clinical application. The validation of the online tremor suppression on more patients with broader range of tremor severity is still required.

In conclusion, the online decomposition-based convolution kernel compensation algorithm was validated with high-density surface EMG recordings of ET patients showing equivalent accuracy of the MU spike trains discrimination to the use of the offline decomposition technique. The application of the PLL to those decomposed MU spike trains shows a promising performance for the tracking of the antagonist muscles phase difference during postural tremor. The proposed

system was preliminarily integrated with a stimulator for a complete verification of the closed-loop working principle.

REFERENCES

[1] K. E. Lyons and R. Pahwa, *Handbook of Essential Tremor and Other Tremor Disorders*. Boca Raton, FL, USA: Taylor & Francis Group, 2005.

[2] G. Deuschl, P. B. Ma, and M. Brin, "Consensus statement of the movement disorder society on tremor," *Movement Disorders*, vol. 13, no. S3, pp. 2–23, 1998.

[3] R. J. Elble and J. E. Randall, "Motor-unit activity responsible for 8-to 12-Hz component of human physiological finger tremor," *J. Neurophysiol.*, vol. 39, no. 2, pp. 370–383, Mar. 1976, doi: 10.1152/jn.1976.39.2.370.

[4] R. J. Elble, "Characteristics of physiologic tremor in young and elderly adults," *Clin. Neurophysiol.*, vol. 114, no. 4, pp. 624–635, 2003, doi: 10.1016/S1388-2457(03)00006-3.

[5] C. W. Hess and S. L. Pullman, "Tremor: Clinical phenomenology and assessment techniques," *Tremor Other Hyperkinetic Movements*, vol. 2, pp. 1–15, Jun. 2012, doi: 10.7916/D8WM1C41.

[6] D. Zhang, P. Poignet, A. P. Bo, and W. T. Ang, "Exploring peripheral mechanism of tremor on neuromusculoskeletal model: A general simulation study," *IEEE Trans. Biomed. Eng.*, vol. 56, no. 10, pp. 2359–2369, Oct. 2009.

[7] Y. Yang, T. Solis-Escalante, M. van de Ruit, F. C. T. van der Helm, and A. C. Schouten, "Nonlinear coupling between cortical oscillations and muscle activity during isotonic wrist flexion," *Frontiers Comput. Neurosci.*, vol. 10, pp. 1–11, Dec. 2016, doi: 10.3389/fncom.2016.00126.

[8] J. Raethjen, R. B. Govindan, M. Muthuraman, F. Kopper, J. Volkmann, and G. Deuschl, "Cortical correlates of the basic and first harmonic frequency of parkinsonian tremor," *Clin. Neurophysiol.*, vol. 120, no. 10, pp. 1866–1872, Oct. 2009, doi: 10.1016/j.clinph.2009.06.028.

[9] J. A. Gallego *et al.*, "Influence of common synaptic input to motor neurons on the neural drive to muscle in essential tremor," *J. Neurophysiol.*, vol. 113, no. 1, pp. 182–191, 2015, doi: 10.1152/jn.00531.2014.

[10] J. Raethjen, R. B. Govindan, F. Kopper, M. Muthuraman, and G. Deuschl, "Cortical involvement in the generation of essential tremor," *J. Neurophysiol.*, vol. 97, no. 5, pp. 3219–3228, May 2007, doi: 10.1152/jn.00477.2006.

[11] B. Hellwig, B. O. Schelter, B. Guschlbauer, J. Timmer, and C. H. Lücking, "Dynamic synchronisation of central oscillators in essential tremor," *Clin. Neurophysiol.*, vol. 114, no. 8, pp. 1462–1467, 2003, doi: 10.1016/S1388-2457(03)00116-0.

[12] G. Puttaraksa *et al.*, "Voluntary and tremorogenic inputs to motor neuron pools of agonist/antagonist muscles in essential tremor patients," *J. Neurophysiol.*, vol. 122, no. 5, pp. 2043–2053, Nov. 2019, doi: 10.1152/jn.00407.2019.

[13] A. M. Amjad, D. M. Halliday, J. R. Rosenberg, and B. A. Conway, "An extended difference of coherence test for comparing and combining several independent coherence estimates: Theory and application to the study of motor units and physiological tremor," *J. Neurosci. Methods*, vol. 73, no. 1, pp. 69–79, 1997, doi: 10.1016/S0165-0270(96)02214-5.

[14] G. K. Wenning *et al.*, "Prevalence of movement disorders in men and women aged 50–89 years (Bruneck study cohort): A population-based study," *Lancet Neurol.*, vol. 4, no. 12, pp. 815–820, 2005, doi: 10.1016/S1474-4422(05)70226-X.

[15] D. Lorenz and G. Deuschl, "Update on pathogenesis and treatment of essential tremor," *Current Opinion Neurol.*, vol. 20, no. 4, pp. 447–452, Aug. 2007, doi: 10.1097/WCO.0b013e3281e66942.

[16] A. C. Pigg *et al.*, "Distribution of tremor among the major degrees of freedom of the upper limb in subjects with essential tremor," *Clin. Neurophysiol.*, vol. 131, no. 11, pp. 2700–2712, Nov. 2020, doi: 10.1016/j.clinph.2020.08.010.

[17] E. D. Louis, "The primary type of tremor in essential tremor is kinetic rather than postural: Cross-sectional observation of tremor phenomenology in 369 cases," *Eur. J. Neurol.*, vol. 20, no. 4, pp. 725–727, Apr. 2013, doi: 10.1111/j.1468-1331.2012.03855.x.

[18] T. A. Zesiewicz, R. Elble, E. D. Louis, W. G. Ondo, G. S. Gronseth, and W. J. Weiner, "Practice parameter?: Therapies for essential tremor," *Amer. Acad. Neurol.*, vol. 64, no. 12, pp. 2008–2020, 2005.

[19] T. C. Britton, P. D. Thompson, B. L. Day, J. C. Rothwell, L. J. Findley, and C. D. Marsden, "Resetting of postural tremors at the wrist with mechanical stretches in Parkinson's disease, essential tremor, and normal subjects mimicking tremor," *Ann. Neurol.*, vol. 31, no. 5, pp. 507–514, May 1992, doi: 10.1002/ana.410310508.

[20] R. J. Elble, C. Higgins, and C. J. Moody, "Stretch reflex oscillations and essential tremor," *J. Neurol., Neurosurg. Psychiatry*, vol. 50, no. 6, pp. 691–698, Jun. 1987, doi: 10.1136/jnnp.50.6.691.

[21] A. Pascual-Leone, J. Valls-Solé, C. Toro, E. M. Wassermann, and M. Hallett, "Resetting of essential tremor and postural tremor in Parkinson's disease with transcranial magnetic stimulation," *Muscle Nerve*, vol. 17, no. 7, pp. 800–807, Jul. 1994.

[22] M. Hallett, "Transcranial magnetic stimulation: A primer," *Neuron*, vol. 55, no. 2, pp. 187–199, Jul. 2007, doi: 10.1016/j.neuron.2007.06.026.

[23] M.-K. Lu, S.-M. Chiou, U. Ziemann, H.-C. Huang, Y.-W. Yang, and C.-H. Tsai, "Resetting tremor by single and paired transcranial magnetic stimulation in Parkinson's disease and essential tremor," *Clin. Neurophysiol.*, vol. 126, no. 12, pp. 2330–2336, Dec. 2015, doi: 10.1016/j.clinph.2015.02.010.

[24] T. C. Britton, P. D. Thompson, B. L. Day, J. C. Rothwell, L. J. Findley, and C. D. Marsden, "Modulation of postural tremors at the wrist by supramaximal electrical median nerve shocks in essential tremor, Parkinson's disease and normal subjects mimicking tremor," *J. Neurol., Neurosurg. Psychiatry*, vol. 56, no. 10, pp. 1085–1089, Oct. 1993, doi: 10.1136/jnnp.56.10.1085.

[25] P. T. Lin *et al.*, "Noninvasive neuromodulation in essential tremor demonstrates relief in a sham-controlled pilot trial," *Movement Disorders*, vol. 33, no. 7, pp. 1182–1183, Jul. 2018, doi: 10.1002/mds.27350.

[26] R. Pahwa *et al.*, "An acute randomized controlled trial of noninvasive peripheral nerve stimulation in essential tremor," *Neuromodulation, Technol. Neural Interface*, vol. 22, no. 5, pp. 537–545, Jul. 2019, doi: 10.1111/ner.12930.

[27] S. H. Isaacson *et al.*, "Prospective home-use study on non-invasive neuromodulation therapy for essential tremor," *Tremor Other Hyperkinetic Movements*, vol. 10, no. 1, pp. 1–16, 2020, doi: 10.5334/tohm.59.

[28] A. Prochazka, J. Elek, and M. Javidan, "Attenuation of pathological tremors by functional electrical stimulation I: Method," *Ann. Biomed. Eng.*, vol. 20, no. 2, pp. 205–224, 1992, doi: 10.1007/BF02368522.

[29] J. L. Dideriksen, F. Gianfelici, L. Z. P. Maneski, and D. Farina, "EMG-based characterization of pathological tremor using the iterated Hilbert transform," *IEEE Trans. Biomed. Eng.*, vol. 58, no. 10, pp. 2911–2921, Oct. 2011, doi: 10.1109/TBME.2011.2163069.

[30] L. P. Maneski *et al.*, "Electrical stimulation for the suppression of pathological tremor," *Med. Biol. Eng. Comput.*, vol. 49, pp. 1187–1193, Oct. 2011, doi: 10.1007/s11517-011-0803-6.

[31] J. L. Dideriksen *et al.*, "Electrical stimulation of afferent pathways for the suppression of pathological tremor," *Frontiers Neurosci.*, vol. 11, pp. 1–11, Apr. 2017, doi: 10.3389/fnins.2017.00178.

[32] D. Zhang, P. Poignet, F. Widjaja, and W. T. Ang, "Neural oscillator based control for pathological tremor suppression via functional electrical stimulation," *Control Eng. Pract.*, vol. 19, no. 1, pp. 74–88, 2011, doi: 10.1016/j.conengprac.2010.08.009.

[33] S. Muceli *et al.*, "A thin-film multichannel electrode for muscle recording and stimulation in neuroprosthetics applications," *J. Neural Eng.*, vol. 16, no. 2, Apr. 2019, Art. no. 026035, doi: 10.1088/1741-2552/ab047a.

[34] A. Pascual Valdunciel *et al.*, "Intramuscular stimulation of muscle afferents attains prolonged tremor reduction in essential tremor patients," *IEEE Trans. Biomed. Eng.*, vol. 68, no. 6, pp. 1–9, Jun. 2020, doi: 10.1109/tbme.2020.3015572.

[35] J. Á. Gallego, E. Rocon, J. M. Belda-Lois, and J. L. Pons, "A neuroprosthesis for tremor management through the control of muscle co-contraction," *J. Neuroeng. Rehabil.*, vol. 10, no. 1, p. 36, 2013, doi: 10.1186/1743-0003-10-36.

[36] S. Dosen *et al.*, "Online tremor suppression using electromyography and low-level electrical stimulation," *IEEE Trans. Neural Syst. Rehabil. Eng.*, vol. 23, no. 3, pp. 385–395, May 2015, doi: 10.1109/TNSRE.2014.2328296.

[37] A. Pascual-Valdunciel *et al.*, "Peripheral electrical stimulation to reduce pathological tremor: A review," *J. Neuroeng. Rehabil.*, vol. 18, no. 1, pp. 1–19, Dec. 2021, doi: 10.1186/s12984-021-00811-9.

[38] J. A. Gallego *et al.*, "The phase difference between neural drives to antagonist muscles in essential tremor is associated with the relative strength of supraspinal and afferent input," *J. Neurosci.*, vol. 35, no. 23, pp. 8925–8937, Jun. 2015, doi: 10.1523/JNEUROSCI.0106-15.2015.

[39] J. L. Dideriksen, R. M. Enoka, and D. Farina, "A model of the surface electromyogram in pathological tremor," *IEEE Trans. Biomed. Eng.*, vol. 58, no. 8, pp. 2178–2185, Aug. 2011, doi: 10.1109/TBME.2011.2118756.

[40] V. Glaser, A. Holobar, and D. Zazula, "Real-time motor unit identification from high-density surface EMG," *IEEE Trans. Neural Syst. Rehabil. Eng.*, vol. 21, no. 6, pp. 949–958, Nov. 2013, doi: 10.1109/TNSRE.2013.2247631.

[41] D. Farina, A. Holobar, R. Merletti, and R. M. Enoka, "Decoding the neural drive to muscles from the surface electromyogram," *Clin. Neurophysiol.*, vol. 121, no. 10, pp. 1616–1623, Oct. 2010, doi: 10.1016/j.clinph.2009.10.040.

[42] A. Holobar and D. Zazula, "Multichannel blind source separation using convolution kernel compensation," *IEEE Trans. Signal Process.*, vol. 55, no. 9, pp. 4487–4496, Sep. 2007, doi: 10.1109/TSP.2007.896108.

[43] A. Holobar and D. Zazula, "Surface EMG decomposition using a novel approach for blind source separation," *Inf. Med. Slovenica*, vol. 8, no. 1, pp. 2–14, 2003.

[44] E. E. Fetz and P. D. Cheney, "Postspike facilitation of forelimb muscle activity by primate corticomotoneuronal cells," *J. Neurophysiology*, vol. 44, no. 4, pp. 751–772, Oct. 1980, doi: 10.1152/jn.1980.44.4.751.

[45] A. Holobar, M. A. Minetto, and D. Farina, "Accurate identification of motor unit discharge patterns from high-density surface EMG and validation with a novel signal-based performance metric," *J. Neural Eng.*, vol. 11, no. 1, pp. 1–11, 2014, doi: 10.1088/1741-2560/11/1/016008.

[46] F. Negro and D. Farina, "Factors influencing the estimates of correlation between motor unit activities in humans," *PLoS ONE*, vol. 7, no. 9, Sep. 2012, Art. no. e44894, doi: 10.1371/journal.pone.0044894.

[47] J. L. Ong *et al.*, "Effects of phase-locked acoustic stimulation during a nap on EEG spectra and declarative memory consolidation," *Sleep Med.*, vol. 20, pp. 88–97, Apr. 2016, doi: 10.1016/j.sleep.2015.10.016.

[48] F. M. Gardner, "Charge-pump phase-lock loops," *IEEE Trans. Commun.*, vol. COM-28, no. 11, pp. 1849–1858, Nov. 1980.

[49] D. Y. Barsakcioglu, M. Bracklein, A. Holobar, and D. Farina, "Control of spinal motoneurons by feedback from a non-invasive real-time interface," *IEEE Trans. Biomed. Eng.*, vol. 68, no. 3, pp. 926–935, Mar. 2021, doi: 10.1109/tbme.2020.3001942.

[50] Y.-W. Liu, "Hilbert transform and applications," in *Fourier Transform Applications*. London, U.K.: IntechOpen, 2012, pp. 291–300, doi: 10.5772/37727.

[51] A. Holobar, V. Glaser, J. A. Gallego, J. L. Dideriksen, and D. Farina, "Non-invasive characterization of motor unit behaviour in pathological tremor," *J. Neural Eng.*, vol. 9, no. 5, pp. 1–13, 2012, doi: 10.1088/1741-2560/9/5/056011.

[52] C. N. Christakos, S. Erimaki, E. Anagnostou, and D. Anastasopoulos, "Tremor-related motor unit firing in Parkinson's disease: Implications for tremor genesis," *J. Physiol.*, vol. 587, no. 20, pp. 4811–4827, Oct. 2009, doi: 10.1113/jphysiol.2009.173989.

[53] A. D. Gupta, "Paired response of motor units during voluntary contraction in parkinsonism," *J. Neurol., Neurosurg. Psychiatry*, vol. 26, no. 3, pp. 265–268, Jun. 1963, doi: 10.1136/jnnp.26.3.265.

[54] K. G. Keenan, D. Farina, K. S. Maluf, R. Merletti, and R. M. Enoka, "Influence of amplitude cancellation on the simulated surface electromyogram," *J. Appl. Physiol.*, vol. 98, no. 1, pp. 120–131, Jan. 2005, doi: 10.1152/japplphysiol.00894.2004.

[55] J. Alcazar, R. Csapo, I. Ara, and L. M. Alegre, "On the shape of the force-velocity relationship in skeletal muscles: The linear, the hyperbolic, and the double-hyperbolic," *Frontiers Physiol.*, vol. 10, pp. 1–21, Jun. 2019, doi: 10.3389/fphys.2019.00769.

[56] Ş. U. Yavuz, A. Şendemir-Ürkmez, and K. S. Türker, "Effect of gender, age, fatigue and contraction level on electromechanical delay," *Clin. Neurophysiol.*, vol. 121, pp. 1700–1706, Oct. 2010, doi: 10.1016/j.clinph.2009.10.039.

[57] G. Drost, D. F. Stegeman, B. G. M. van Engelen, and M. J. Zwarts, "Clinical applications of high-density surface EMG: A systematic review," *J. Electromyogr. Kinesiol.*, vol. 16, pp. 586–602, Dec. 2006, doi: 10.1016/j.jelekin.2006.09.005.

[58] D. Farina, F. Negro, S. Muceli, and R. M. Enoka, "Principles of motor unit physiology evolve with advances in technology," *Physiology*, vol. 31, no. 2, pp. 83–94, Mar. 2016, doi: 10.1152/physiol.00040.2015.

[59] R. Merletti, A. Holobar, and D. Farina, "Analysis of motor units with high-density surface electromyography," *J. Electromyogr. Kinesiol.*, vol. 18, pp. 879–890, Dec. 2008, doi: 10.1016/j.jelekin.2008.09.002.

[60] M. Chen, A. Holobar, X. Zhang, and P. Zhou, "Progressive FastICA peel-off and convolution kernel compensation demonstrate high agreement for high density surface EMG decomposition," *Neural Plasticity*, vol. 2016, pp. 1–5, Aug. 2016, doi: 10.1155/2016/3489540.

[61] F. Negro, S. Muceli, A. M. Castronovo, A. Holobar, and D. Farina, "Multi-channel intramuscular and surface EMG decomposition by convolutive blind source separation," *J. Neural Eng.*, vol. 13, no. 2, Apr. 2016, Art. no. 026027, doi: 10.1088/1741-2560/13/2/026027.

[62] A. Holobar, M. A. Minetto, A. Botter, F. Negro, and D. Farina, "Experimental analysis of accuracy in the identification of motor unit spike trains from high-density surface EMG," *IEEE Trans. Neural Syst. Rehabil. Eng.*, vol. 18, no. 3, pp. 221–229, Jun. 2010, doi: 10.1109/TNSRE.2010.2041593.